Gas Holdup in a Three-Phase Fluidized Bed

M. Safoniuk and J. R. Grace
Dept. of Chemical and Bio-Resource Engineering, University of British Columbia, Vancouver, Canada V6T 1Z4

L. Hackman and C. A. McKnight
Syncrude Research Centre, Edmonton, Alberta, Canada T6N 1H4

For chemical processes where mass transfer is the rate-limiting step, it is important to be able to estimate the gas holdup as this relates directly to the mass transfer (Fan, 1989). Although gas holdup in three-phase fluidized beds has received significant attention, as summarized in various reviews (Epstein, 1981; Wild et al., 1984; Darton, 1985; Muroyama and Fan, 1985; Fan, 1989; Nacef et al., 1992; Wild and Poncin, 1969; Kim and Kang, 1997), most previous work has utilized air, water, and small glass beads as the gas, liquid, and solids, respectively. This combination limits the generality and usefulness of the results. The gas holdup in such systems is often considerably lower than for pilot-plant or industrial-scale units (Tarmy et al., 1984a,b). Most researchers attribute this difference to air, water, and glass beads having physical properties which differ considerably from those typically found in industrial processes. These processes are often operated at much higher temperatures and pressures than those used in the traditional air-water-glass beads experimental systems.

In a previous article (Safoniuk et al., 1999), a series of five dimensionless operating groups ($M = g\Delta\rho\mu_L^4/(\rho_L^2\sigma^3)$, $Eo = g\Delta\rho d_p^2/\sigma$, $Re_L = \rho_L d_p U_L/\mu_L$, $\beta_d = \rho_p/\rho_L$; and $\beta_u = U_g/U_L$) was proposed for cold modeling of many three-phase systems, based upon the principle of dynamic similarity, subject to certain restrictions ($\rho_L \gg \rho_g$; $D \gg d_p$). By matching these five groups, the operating conditions in a small-scale unit could be set such that the unit should operate in a dynamically similar manner to a given industrial reactor. Average gas holdups were measured with the aid of a conductivity probe for a series of operating conditions, using, as a starting point, the operating conditions of an ebullated-bed industrial reactor. In addition, radial profiles of the gas holdup were obtained for several operating conditions.

Experimental Equipment

An acrylic column commissioned for this work is shown in Figure 1. The column has an inside diameter of 292 mm and allows ebullated bed heights up to 1.8 m. Ports at 0.10 m intervals along the column can be connected to pressure barometers or used for insertion of a conductivity point probe.

The distributor system was designed based upon commonly used methods for gas-solid fluidized beds (for example, see Kunii and Levenspiel (1969)). To distribute the gas into the liquid, a ring with thirty 3.2-mm holes through which the gas passed into the liquid was placed in the middle of the pre-mix chamber below the distributor plate. Initial tests with no particles and a stagnant height of 0.30 m of water above the distributor indicated that the gas was uniformly dispersed within the water. The distributor plate was designed to support the particles when at rest and to distribute the gas-liquid mixture. If the gas-liquid mixture is considered as a homogeneous fluid and the hole diameter is 6.3 mm, the Kunii and Levenspiel (1969) method suggests that 236 holes are required to distribute the solids and gas-liquid mixture properly, and this was adopted for the distributor plate. The premix chamber was filled with 13-mm Raschig rings to further enhance distribution. Tests with liquid flow alone resulted in a smooth bed-freeboard region interface, suggesting that the distributor plate achieved a good distribution of the liquid.

The liquid, gas, and solids used in the experiments were carefully selected to ensure that the dimensionless operating groups were well matched to those in the industrial unit. Due to its ready availability, air was chosen as the gas. The air superficial velocity was controlled with a Hedland valve and varied between 0 and 0.15 m/s.

The liquid entered at the base of the column and was recovered after overflowing at the top of the column and returned to a solution storage tank, as indicated in Figure 1. Its flow was controlled by means of a large ball valve. An orifice meter and a differential pressure transducer were used to monitor the liquid superficial velocity between 0 and 0.22 m/s. Three different liquids were used: tap water, an aqueous 44% by mass glycerol solution, and a more concentrated aqueous 60% by mass glycerol solution. The pertinent physical properties of these liquids appear in Table 1 for the set point temperatures given the more viscous solutions requiring higher temperatures due to viscous dissipation.

The particles, selected to achieve dynamic similarity and maintain geometric similarity with an industrial ebullated bed

Current address of M. Safoniuk: Southern Alberta Institute of Technology, Energy Dept., Calgary, Alberta, Canada T2M0L4.

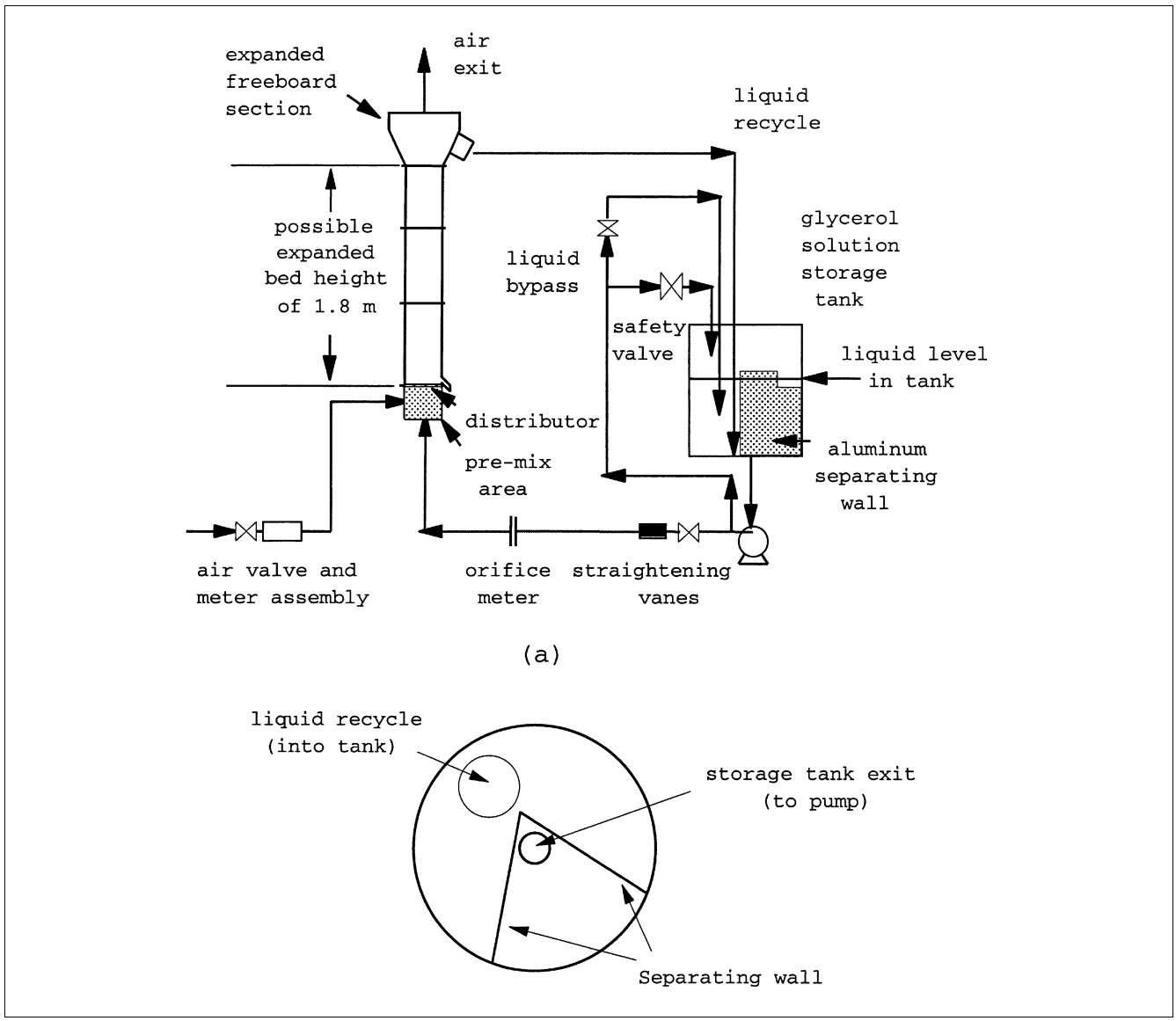

Figure 1. Experimental column.

(a) Overall setup; (b) overhead view of storage tank.

unit, were aluminum cylinders, 4 mm in diameter and 10 mm in length (with a spherical volume-equivalent diameter of 6.2 mm). The ratio of the particle diameter (or length) to the column diameter was not maintained the same as in the full-scale unit, but was small enough that wall effects are expected to be of little consequence in both cases. In each sys-

Table 1. Physical Properties of Liquids and Operating Temperatures

Liquid	Temp. (°C)	μ_L (Pa·s)	σ (kg/s^2)	ρ_L (kg/m^3)	U_{lmf} (m/s)*	U_t (m/s)**
Tap water	12 ± 0.2	1.2×10^{-3}	72×10^{-3}	999	0.0585	0.303
44 Mass % (by wt.) aqueous glycerol	21 ± 0.4	4.5×10^{-3}	67.4×10^{-3}	1,097	0.0417	0.289
60 Mass % (by wt.) glycerol solution	24 ± 0.5	11.5×10^{-3}	66.8×10^{-3}	1,150	0.0248	0.261

*From correlation of Wen and Yu (1966)
**From equations presented in Clift et al. (1978)

tem, operation is in the dispersed bubble flow regime, with bubble volume-equivalent diameters, again, much smaller than the column diameter. The ranges of the five key dimensionless groups were such that they covered the values pertaining to the industrial unit.

Measurement Techniques

To obtain average gas holdups across the ebullated bed, pressure drops were measured across the bed height. Assuming negligible acceleration and wall friction, the measured pressure drop is related directly to the density of the individual phases by

$$\frac{\Delta P}{g\Delta z} = \rho_g \epsilon_g + \rho_L \epsilon_L + \rho_p \epsilon_p \tag{1}$$

The solids holdup can be calculated based on the overall bed expansion and the known solids loading of the bed

$$\epsilon_p = \frac{W_s}{\rho_p A H_e} \tag{2}$$

Since the only phases present in the reactor are the gas, liquid, and particles

$$\epsilon_g + \epsilon_L + \epsilon_p = 1 \tag{3}$$

Equations 1, 2, and 3 constitute three equations in three unknowns, and, hence, allow the overall gas holdup to be estimated.

A specially built conductivity probe was used to measure radial profiles of the local gas holdup at different heights and operating conditions. The probe is shown in Figure 2. The essential components are two lengths of 1.0-mm dia. standard electrical copper wire and the stainless steel shaft through which they pass. The wires are coated with Teflon to insulate them electrically from one another and from the probe shaft. The tips are uncovered to allow sensing of the conductivity surrounding them. The probe is tapered, reducing in diameter from 7.9 to 3.2 mm near the tip, making the probe less instrusive in the vicinity of the measurements. The two sensors of the conductivity probe are attached to two Wheatstone bridges across which voltages are measured. The probe has two tips to allow measurement of bubble velocities and pierced chord lenghts. For gas holdups, only a single tip is required. A typical signal from one tip of the conductivity probe, as recorded on a Pentium computer using specially written software, is shown in Figure 3. The top signal corresponds to the raw data, while the lower signal is the result after filtering to eliminate the low-frequency base line fluctuation. The signal base line is shown superimposed on the top curve as a thicker lighter line. When the liquid alone surrounds the probe, the signal has a value of approximately 2.4 volts. When gas, in the form of bubbles, surrounds the probe tip, the signal drops towards zero. At times, particles in the vicinity of the probe touch the probe, causing upward spikes. A threshold value was set following calibration of the probe (see Safoniuk et al. (1999) for details). Any signal below the threshold value was considered to indicate gas surrounding the probe tip. The gas holdup is then equal to the fraction of the time that the signal is below the threshold value.

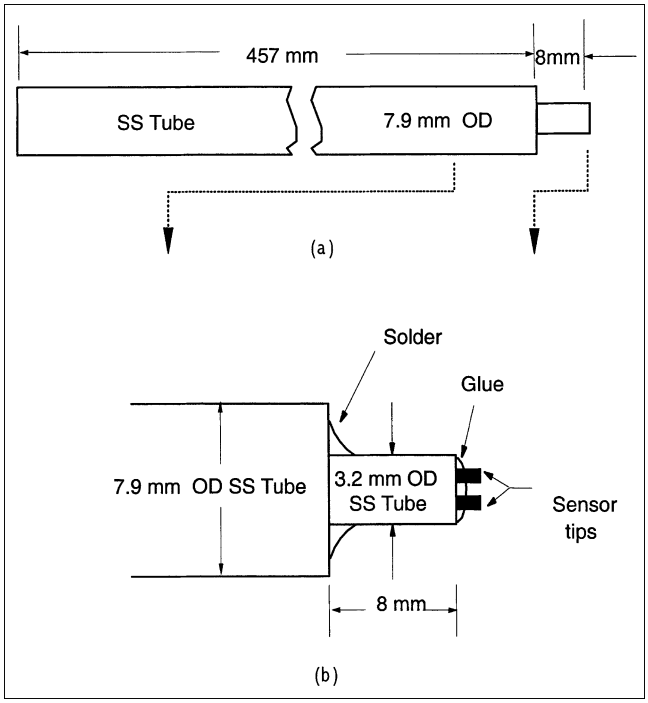

Figure 2. Two-tip conductivity probe.
(a) Overall; (b) details of sensing end.

Tap water experiments

The gas holdups measured in the aluminum cylinder/water/air system are shown in Figure 4. To obtain local values, these measurements were obtained using the conductiv-

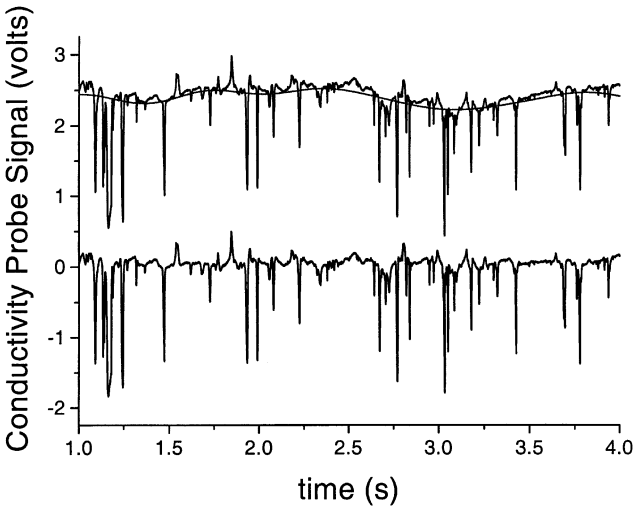

Figure 3. Conductivity probe signal from lower probe tip before (top) and after (bottom) processing through fast fourier transform subroutine.
Liquid is 44% by mass aqueous glycerol. $Re_g = 105$, $Re_L = 117$, $M = 1.20 \times 10^{-8}$, $Eo = 2.55$, $\beta_d = 2.46$, $W_S = 25.5$ kg, Probe tip at $z = 0.05$ m, $r/R = 0.863$.

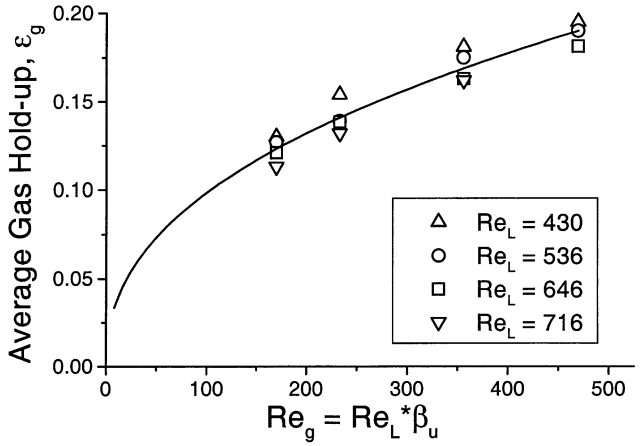

Figure 4. Average gas holdup vs. modified gas Reynolds number ($\beta_u Re_L$) for various liquid Reynolds numbers.

Holdups were determined by integrating conductivity probe local measurements with tap water and air as the fluids. $M = 5.46 \times 10^{-11}$, $Eo = 2.18$, $\beta_d = 2.75$, and $W_s = 53.4$ kg. The line shown corresponds to Eq. 5.

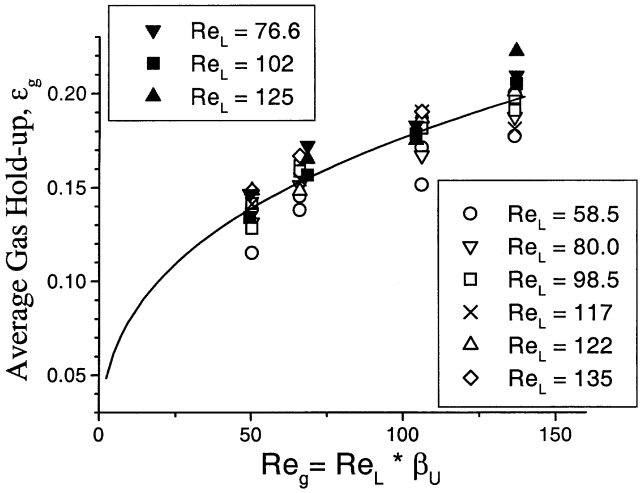

Figure 5. Average gas hold-up, determined from pressure drops vs. modified gas Reynolds number for various liquid Reynolds number with aqueous 44 mass % glycerol solution as the liquid.

$M = 1.20 \times 10^{-8}$, $Eo = 2.55$, $\beta_d = 2.46$, $W_s = 53.4$ kg. The line shown corresponds to Eq. 6.

ity probe. However, using the conductivity probe yields local measurements, the data had to be integrated over the column cross-section to yield average gas holdups at each measurement height, that is

$$\bar{\epsilon}_g = \frac{1}{A}\int_0^{D/2} \epsilon_g(r) 2\pi r dr \tag{4}$$

Gas holdups calculated with Eq. 4 should be equal to those measured by the pressure drop method provided: (a) a complete radial profile is available so that local zones of high or low gas concentration are included in the calculations; and (b) bubbles are not deflected by the probe tip. In case the latter proves untrue, a slightly lower gas holdup would be calculated with Eq. 4 than measured using the pressure drop. From Figure 4, it is evident that the gas holdup depends strongly on the modified gas Reynolds number. This trend, which was observed for all three liquids, is correctly predicted by the correlation of Bloxom et al. (1975). Clearly in Figure 4, there is also a slight increase in the measured holdup with a decreasing liquid Reynolds number, again consistent with the correlation. While the correlation of Bloxom et al. (1975) is identified by Wild and Poncin (1996) as the best available for gas holdups, it can have a deviation greater than 40% when compared to other data. In this case, the correlation predicts gas holdups in the range of 0.069 to 0.160, slightly lower than the measured values.

The results were fitted to a power-law equation passing through the origin (zero gas holdup at zero gas flow) with no dependence on liquid Reynolds number. For the tap water system ($M = 5.94 \times 10^{-11}$, $Eo = 2.24$, $\beta_d = 2.70$, $430 \le Re_L \le 716$), this led to

$$\epsilon_g = 0.0139 Re_g^{0.426} \tag{5}$$

(with a standard deviation of 0.000718 and a correlation factor of 0.95).

44% by mass aqueous glycerol solution experiments

Figure 5 shows measured gas holdups with an aqueous 44 mass % glycerol solution as the liquid. For this set of experiments, a bank of pressure barometers was used to obtain pressure drop measurements. As in the water system, the holdup is directly related to the gas Reynolds number. However, unlike the situation with water, there seems to be little or no effect of liquid Reynolds number.

For the aqueous 44 mass % glycerol solution, the correlation of Bloxom et al. (1975) predicts gas holdups in the range of 0.075 to 0.172. As in the case of the tap water experiments, the predictions fall slightly below the measured values, but are well within the $\pm 40\%$ deviation anticipated (Wild and Poncin, 1996).

These data were correlated (for the range of conditions $M = 12.0 \times 10^{-8}$, $Eo = 2.55$, $\beta_d = 2.46$, $73 \le Re_L \le 156$) by

$$\epsilon_g = 0.0359 Re_g^{0.346} \tag{6}$$

(with a standard deviation of 0.00183 and a correlation factor of 0.89).

The open data points in Figure 5 are from a set of early experiments in which the gas holdup was measured by pressure difference in the freeboard region immediately above the three-phase fluidized-bed region. These results were checked using a conductivity probe inserted just below the interface and the measurements agreed quite well, suggesting that, for the conditions studied, the gas holdup immediately above the three-phase fluidized-bed region is similar to that in the bed. The solid data points in Figure 5 also indicate

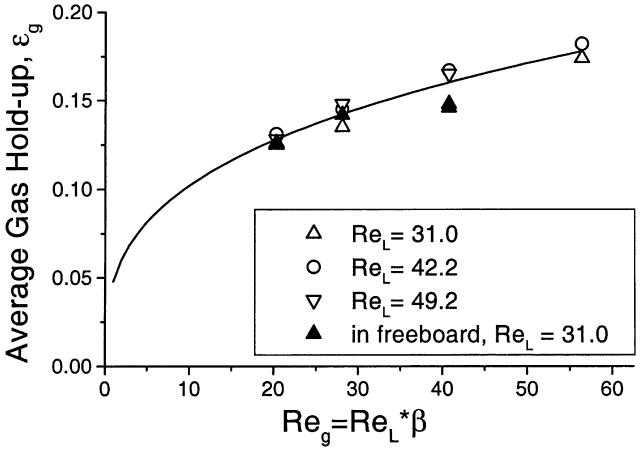

Figure 6. Average gas holdup determined from pressure drops, vs. modified gas Reynolds number for various liquid Reynolds number values.

Experiments conducted with a concentrated (60 mass %) aqueous glycerol solution and air as the fluids. Fluid properties are listed. $M = 5.01 \times 10^{-7}$, $Eo = 2.70$, $\beta_d = 2.35$, $W_s = 53.4$ kg. The line shown corresponds to Eq. 7.

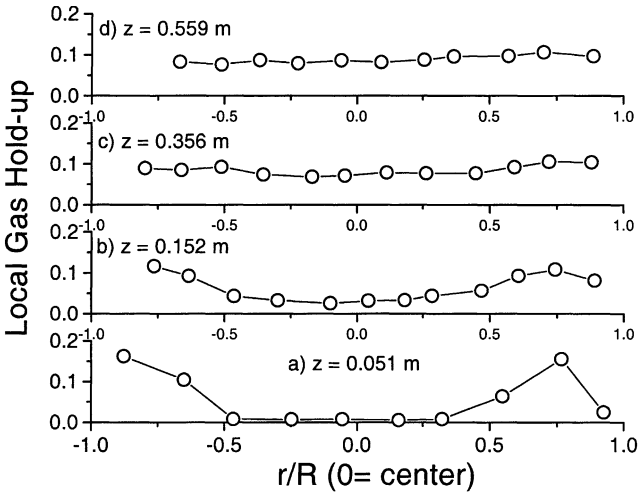

Figure 7. Local gas holdup at various radial positions and four different heights.

Holdups were determined by conductivity probe with a 44 mass % glycerol solution and air as the fluids. $Re_L = 58.5$, $Re_g = 49.6$, $M = 1.20 \times 10^{-8}$, $Eo = 2.55$, $\beta_d = 2.46$, $W_s = 53.4$ kg.

this. These points represent results from pressure measurements across as much of the height of the fluidized bed as possible (using pressure differentials between the port closest to the bed surface and the lowest port) and they are consistent with the earlier data. Note that these two series of experiments were conducted for two separate batches of aqueous 44 mass % glycerol solution, more than two years apart, giving a measure of the reproducibility of the data.

Concentrated aqueous glycerol solution experiments

Figure 6 plots the average gas holdup in the fluidized bed for the most concentrated glycerol solution. The holdups were determined, as for the more dilute glycerol solution, from pressure drop measurements. The results again show no significant dependence of gas holdup on liquid Reynolds number. For the aqueous 60 mass % glycerol solution, the correlation of Bloxom et al. (1975) predicts gas holdups in the range of 0.075 to 0.172. As in the previous cases, these predictions are slightly lower than the measured values, but well within the 40% deviation expected with this correlation.

The open points in Figure 6 represent data from pressure drops within the fluidized bed, while the solid points are for the freeboard immediately above the surface of the three-phase fluidized bed. As in the earlier case, there was little difference between the gas holdups in these two regions. The data were correlated (for the range of condition $M = 5.0 \times 10^{-7}$, $Eo = 2.70$, $\beta_d = 2.35$, $31 \le Re_L \le 50$) by

$$\epsilon_g = 0.0486 Re_g^{0.322} \tag{7}$$

(with a standard deviation of 0.000384 and a correlation factor of 0.95).

Radial profiles of local gas holdup

Figure 7 shows local gas holdups measured by the conductivity probe for the aqueous 44 mass % glycerol solution. This series of experiments was prompted by early work (Safoniuk, 1999) in which the conductivity probe 0.051 m above the distributor plate registered much smaller gas holdups than at greater heights. As shown by Figure 7, the explanation is primarily maldistribution of air at the distributor. At the lowest measurement height of 0.051 m, gas bubbles were found to be restricted to the region near the wall of the column. This maldistribution corrected itself, however, with increasing height. The nonuniformity almost completely disappeared within the lowest 0.36 m of the bed, and was completely eliminated by $z = 0.56$ m. The design of the distributor system was clearly incapable of eliminating the observed maldistribution. Other measures beyond those described above are needed to ensure a uniform distribution of gas at the bottom of the base, such as separate introduction of gas and liquid.

Similar results were obtained with water as the liquid, despite concerted efforts to improve the flow uniformity by increasing the pressure drop in the pre-mix area. Figures 8 through 11 show typical local gas hold-up profiles at different heights for the water experiments. However, in all fifteen cases examined (only five are presented here), the fluidized bed self-corrected the maldistribution completely within 0.56 m of the distributor.

The effect of varying the superficial gas velocity can be determined by comparing Figures 8 through 11. Comparison of Figures 8 and 9 indicates that as the gas Reynolds number increases significantly while Re_L is nearly constant, more gas appears in the central region of the column. However, Figure 10 indicates that this is true only for relatively low liquid Reynolds numbers. At higher liquid velocities, and, hence, higher Re_L, the gas still has difficulty penetrating the inner core of the column at low heights. As seen in Figure 11, at

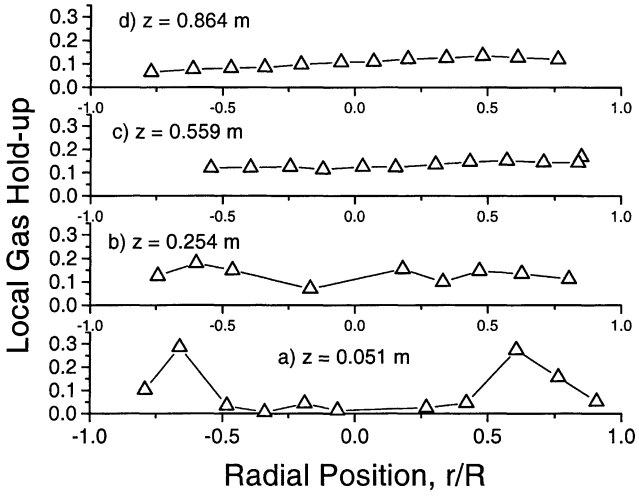

Figure 8. Local gas holdup at various radial positions and four different heights.

Holdups were determined by conductivity probe with tap water and air as the fluids. $Re_L = 430$, $Re_g = 170$, $M = 5.46 \times 10^{-11}$, $Eo = 2.18$, $\beta_d = 2.75$, $W_s = 53.4$ kg.

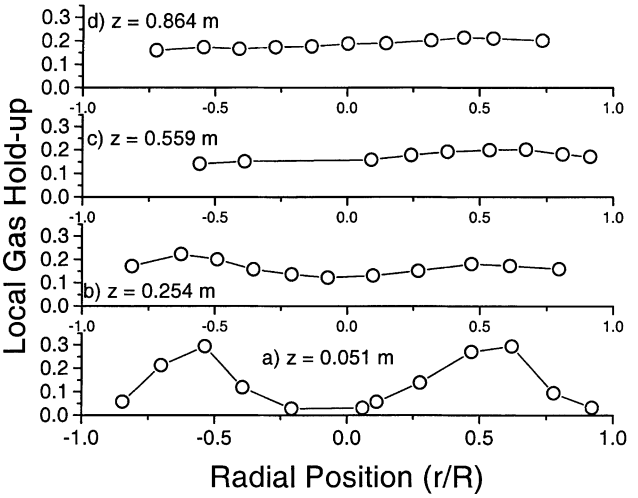

Figure 10. Local gas holdup at various radial positions and four different heights.

Holdups were determined by conductivity probe with tap water and air as the fluids. $Re_L = 536$, $Re_g = 356$, $M = 5.46 \times 10^{-11}$, $Eo = 2.18$, $\beta_d = 2.75$, $W_s = 53.4$ kg.

the lowest measurement height ($z = 0.051$ m), for systems where the gas velocity is considerably lower than the liquid velocity, that is, $Re_L \gg Re_g$, the radial profile is similar to those in Figures 8 and 10.

Conclusions

Gas holdups were measured under various operating conditions, including conditions dynamically similar to those in an industrial reactor, for three different liquid solutions (tap water, aqueous 44 mass % glycerol solution, and aqueous 60 mass % glycerol solution). The overall gas holdup is a strong function of the modified gas Reynolds number.

Radial profiles of the gas holdup show that severe maldistribution can occur at the base of an ebullated bed, despite careful attention to the distributor system design. The results indicate, however, that such maldistribution disappears with increasing height within the bed.

Acknowledgments

The authors are grateful to Syncrude Canada and the Natural Science and Engineering Research Council of Canada (NSERC) for supporting this work.

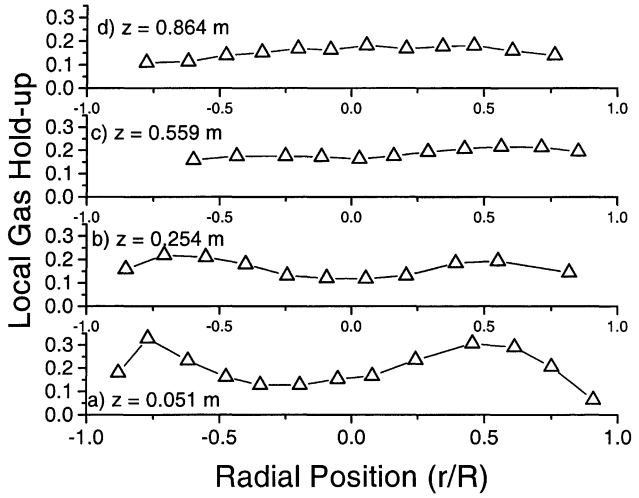

Figure 9. Local gas holdup at various radial positions and four different heights.

Holdups were determined by conductivity probe with tap water and air as the fluids. $Re_L = 430$, $Re_g = 470$, $M = 5.46 \times 10^{-11}$, $Eo = 2.18$, $\beta_d = 2.75$, $W_s = 53.4$ kg.

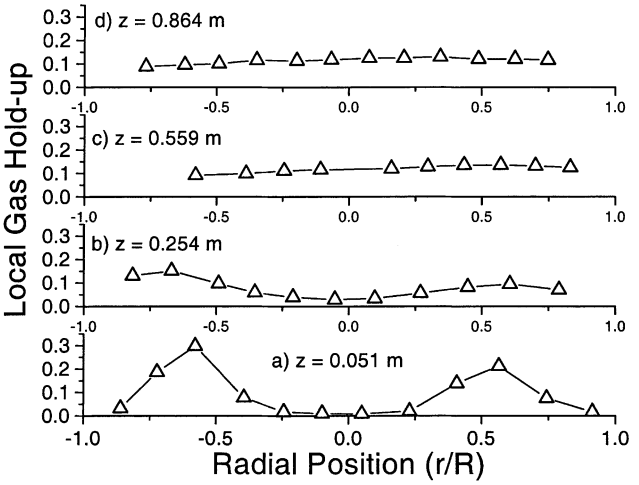

Figure 11. Local gas holdup at various radial positions and four different heights.

Holdups were determined by conductivity probe with tap water and air as the fluids. $Re_L = 716$, $Re_g = 170$, $M = 5.46 \times 10^{-11}$, $Eo = 2.18$, $\beta_d = 2.75$, $W_s = 53.4$ kg.

Notation

A = cross-sectional area, m^2
d_p = particle cylindrical diameter, m
D = column diameter, m
Eo = Eötvös number = $g\Delta\rho d_p^2/\sigma$
g = acceleration due to gravity = 9.81 m/s^2
H_e = expanded bed height, m
H_o = settled bed height, m
M = M-group = $g\mu_L^4/(\rho_L\sigma^3)$
ΔP = pressure drop, Pa
r = radial coordinate, m
Re_g = modified gas Reynolds number = $\beta_u Re_L = \rho_L d_p U_g/\mu_L$
R_{eL} = liquid Reynolds number = $\rho_L d_p U_L/\mu_L$
U = superficial velocity, m/s
U_{lmf} = minimum liquid velocity for liquid-solid fluidization, m/s
U_t = particle terminal velocity, m/s
W_s = particle inventory, kg
z = height above distributor, m
β_d = ratio of densities = ρ_P/ρ_L
β_u = ratio of superficial velocities = U_g/U_L
$\Delta\rho$ = density difference = $\rho_L - \rho_g$, kg/m^3
Δz = height interval, m
ϵ = hold-up (equal to total bed porosity = $\epsilon_g + \epsilon_L$ if no subscript present)
μ = viscosity, Pa·s
ρ = density, kg/m^3
σ = surface tension, kg/s^2

Subscripts

g = gas
L = liquid
p = particle

Literature Cited

Bloxom, V. R., J. M. Costa, J. Herranz, G. L. MacWilliam, and S. R. Roth, "Determination and Correlation of Hydrodynamic Variables in a Three-Phase Fluidized Bed (part IV)," Oak Ridge National Laboratory-MIT, Report no. 219 (1975).

Clift, R., J. R. Grace, and M. E. Weber, *Bubbles, Drops and Particles*, Academic Press, New York (1978).

Darton, R. C., "The Physical Behaviour of Three-Phase Fluidized Beds," *Fluidization*, 2nd ed., J. F. Davidson, R. Clift, and D. Harrison, ed., Academic Press, London, pp. 495–528 (1985).

Epstein, N., "Three-Phase Fluidization: Some Knowledge Gaps," *Can. J. Chem. Eng.*, **59**, 659 (1981).

Fan, L. S., *Gas-Liquid-Solid Fluidization Engineering*, Butterworths, Boston (1989).

Kim, S. D., and Y. Kang, "Heat and Mass Transfer in Three-Phase Fluidized-Bed Reactors—An Overview," *Chem. Eng. Sci.*, **52**, 3639 (1997).

Kunii, D., and O. Levenspiel, *Fluidization Engineering*, Wiley, New York (1969).

Muroyama, K., and L. S. Fan, "Fundamentals of Gas-Solid-Liquid Fluidization," *AIChE J.*, **31**, 1 (1985).

Nacef, S., G. Wild, A. Laurent, and S. D. Kim, "Scale Effects in Gas-Liquid-Solid Fluidization," *Int. Chem. Eng.*, **32**, 51 (1992).

Safoniuk, M., "Dimensional Similitude and the Hydrodynamics of Three-Phase Fluidized Beds," PhD Thesis, University of British Columbia, Vancouver (1999).

Safoniuk, M., J. R. Grace, L. Hackman, and C. A. McKnight, "Use of Dimensional Similitude for Scale-up of Hydrodynamics in Three-phase Fluidized Beds," *Chem. Eng. Sci.*, **54**, 4961 (1999).

Tarmy, B., M. Chang, C. Coulaloglou, and P. Ponzl, "Hydrodynamic Characteristics of Three Phase Reactors," *Chem. Engineer*, 18 (1984a).

Tarmy, B. L., M. Chang, C. A. Coulaloglou, and P. R. Ponzl, "The Three Phase Hydrodynamic Characteristics of the EDS Coal Liquefaction Reactors: Their Development and Use in Reactor Scaleup," *Inst. Chem. Eng. Symposium Series 87*, 303 (1984b).

Wen, C. Y., and Y. H. Yu, "Mechanics of Fluidization," *Chem. Eng. Prog. Symp. Ser.*, **62**, 100 (1966).

Wild, G., and S. Poncin, "Chapter 1: Hydrodynamics," *Three-Phase Sparged Reactors*, K. D. P. Nigam, and A. Schumpe, eds., Gordon and Breach Publishers, Amsterdam (1996).

Wild, G., M. Saberian, J.-L. Schwartz, and J.-C. Charpentier, "Gas-Liquid-Solid Fluidized-Bed Reactors. State of the Art and Industrial Possibilities," *Int. Chem. Eng.*, **24**, 639 (1984).

Manuscript received Apr. 23, 2000, and revision received Jan. 23, 2002.